Solubilities of Carbon Dioxide and Nitrous Oxide in Cyclohexanone, Toluene, and *N,N*-Dimethylformamide at Elevated Pressures

Chiehming J. Chang* and Chiu-Yang Chen†

Department of Chemical Engineering, College of Engineering, National Chung-Hsing University, Taichung, Taiwan 402, Republic of China

Hsi-Chang Lin

Department of Chemical Engineering, Yuan-Ze Institute of Technology, Neili, Taoyuan Shian, Taiwan 320, Republic of China

The solubilities of carbon dioxide and nitrous oxide in three liquid solvents were measured under static phase equilibrium conditions at temperatures of 290.8, 300.9, and 310.1 K and pressures up to 12.34 MPa. The solubility data were determined from the liquid phase density obtained from an Anton-Paar densitometer, and the level of liquid phase expanded by supercritical and subcritical gases. The solubility of N_2O in each solvent increased with pressure, but decreased with temperature, and in each case, was greater than that of CO_2. Both CO_2 and N_2O showed the highest solubility in cyclohexanone and the least solubility in *N,N*-dimethylformamide.

Introduction

The phase behavior of compressed gases in low-volatile solvents has received wide attention in recent years for potential applications in supercritical fluid extraction (*1*−*5*). However, solubilities of high-pressure gases and supercritical fluids in low-volatile organic solvents are scarce in the literature. Elgin and Weinstock (*6*) studied phase equilibria at elevated pressures in ternary systems of ethylene and water with organic liquids. Katayama et al. (*7*) and Weber et al. (*8*) reported vapor and liquid mole fractions for the CO_2 + methanol system at 25 °C. Ng and Robinson (*9*), Morris and Donohue (*10*), Sebastian et al. (*11*), and Fink and Hershey (*12*) measured the phase behavior of toluene + CO_2 at several temperatures. Baumgaertner et al. (*13*) and Clever and Han (*14*), respectively, reviewed the solubilities of light hydrocarbons and noble gases in water from 350 to 600 K at elevated pressures. Japas and Franck (*15*) and Mather and Franck (*16*) measured the phase equilibria of water + O_2 and water + CO_2 at elevated pressures, respectively. Equilibrium phase compositions of CO_2 + decane and CO_2 + methyl linoleate at 40 and 70 °C at pressures from 4.0 to 20.0 MPa (*17*), the solubility of CO_2 in benzaldehyde (*18*), and solubilities of ethylene in benzene, toluene, and isooctane (*19*) were measured previously.

Although some solubility data of CO_2 gas in liquid solvent were reported, few have been studied for the solubility of N_2O in the liquid solvent at elevated pressures. In this work, solubilities of CO_2 and N_2O in cyclohexanone, *N,N*-dimethylformamide, and toluene over the temperature range from 290.8 to 310.1 K at pressures up to 12.34 MPa were measured and correlated by the proposed equations.

Experimental Section

The experimental apparatus is illustrated schematically in Figure 1. The similar experimental techniques for measuring gas solubility in liquids by a densitometer were reported in refs 20−22. The arrangement shown is de-

* To whom correspondence should be addressed.
† Department of Environmental Engineering.

Table 1. Mole Fraction, Liquid Density, and Liquid Volume of CO_2 (1) + Cyclohexanone (2) at 290.8, 300.9, and 310.1 K

P/MPa	x_1	ϱ_L/(g·cm^{-3})	V_L/cm^3
		T = 290.8 K	
1.43	0.239	0.9583	16.9
2.22	0.383	0.9644	18.8
2.51	0.424	0.9666	19.6
2.88	0.493	0.9695	21.1
3.25	0.552	0.9716	22.7
3.58	0.626	0.9734	25.6
3.92	0.680	0.9737	28.5
4.34	0.754	0.9707	34.8
4.64	0.815	0.9628	43.9
4.93	0.871	0.9468	60.4
5.16	0.922	0.9196	97.0
		T = 300.9 K	
1.44	0.210	0.9477	16.6
2.22	0.345	0.9524	18.3
2.56	0.387	0.9541	19.0
2.94	0.453	0.9560	20.2
3.27	0.504	0.9574	21.4
3.62	0.545	0.9587	22.6
3.96	0.580	0.9595	23.8
4.28	0.630	0.9600	25.9
4.64	0.677	0.9596	28.5
4.97	0.718	0.9579	31.5
5.31	0.766	0.9529	36.5
5.66	0.813	0.9456	44.0
5.93	0.857	0.9299	56.0
6.18	0.897	0.9080	76.0
6.36	0.919	0.8905	97.6
		T = 310.1 K	
1.54	0.182	0.9374	16.4
2.27	0.296	0.9404	17.6
2.93	0.372	0.9427	18.7
3.61	0.451	0.9447	20.2
4.28	0.528	0.9460	22.2
4.93	0.603	0.9463	24.8
5.30	0.640	0.9448	26.6
5.68	0.682	0.9431	29.0
6.02	0.718	0.9398	31.8
6.33	0.755	0.9346	35.6
6.71	0.800	0.9243	42.2
7.06	0.844	0.9115	52.4
7.42	0.884	0.8856	69.7
7.79	0.921	0.8522	102.4

0021-9568/95/1740-0850$09.00/0

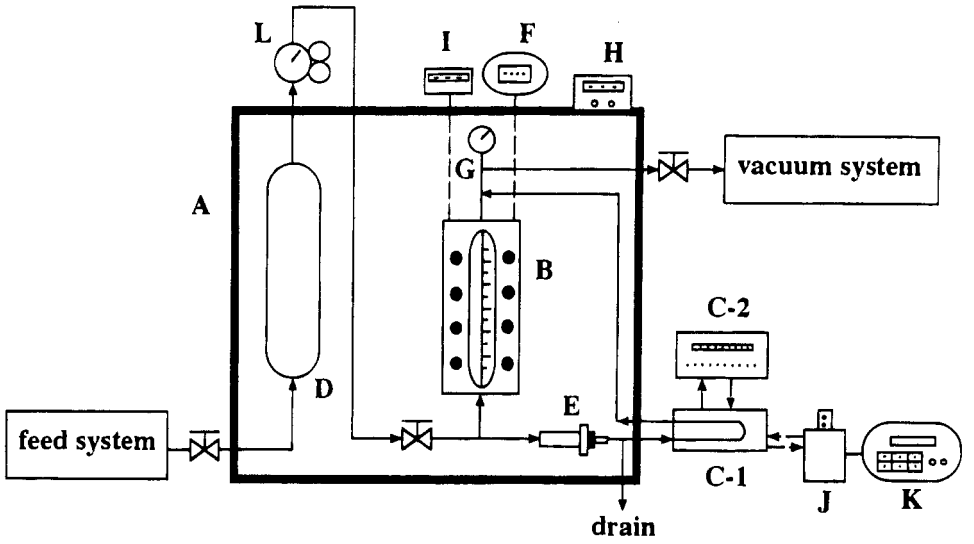

Figure 1. Schematic flow diagram for measurement of equilibrium phase compositions: (A) constant temperature air oven; (B) Jerguson cell; (C) densitometer (1, DMA512; 2, DMA60); (D) storage cylinder; (E) recirculation pump; (F) digital pressure transducer; (G) Bourdon tube gauge; (H) temperature controller; (I) digital temperature indicator; (J) constant temperature bath; (K) high-precision thermometer; (L) feed forward regulator.

Table 2. Mole Fraction, Liquid Density, and Liquid Volume of CO_2 (1) + Toluene (2) at 290.8, 300.9, and 310.1 K

P/MPa	x_1	ϱ_L/(g·cm^{-3})	V_L/cm^3
	T = 290.8 K		
1.44	0.191	0.8752	16.5
2.21	0.285	0.8803	17.6
2.56	0.337	0.8830	18.3
2.91	0.394	0.8858	19.2
3.27	0.464	0.8891	20.7
3.63	0.530	0.8922	22.4
3.98	0.592	0.8945	24.6
4.31	0.686	0.8985	29.6
4.62	0.767	0.8980	37.2
4.89	0.855	0.8902	55.9
5.17	0.922	0.8704	98.3
	T = 300.9 K		
1.16	0.112	0.8654	15.8
2.19	0.237	0.8708	17.0
2.56	0.314	0.8728	18.0
2.95	0.351	0.8751	18.6
3.29	0.393	0.8767	19.3
3.65	0.440	0.8784	20.2
3.96	0.474	0.8801	21.0
4.29	0.527	0.8821	22.4
4.62	0.608	0.8837	25.5
4.99	0.670	0.8843	28.7
5.29	0.742	0.8822	34.7
5.66	0.825	0.8717	48.1
5.91	0.876	0.8558	65.9
6.16	0.917	0.8391	96.4
	T = 310.1 K		
1.17	0.111	0.8542	15.8
2.27	0.225	0.8581	16.9
2.60	0.263	0.8593	17.4
2.99	0.293	0.8608	17.7
3.27	0.331	0.8617	18.3
3.69	0.396	0.8633	19.4
4.00	0.424	0.8643	19.9
4.35	0.443	0.8650	20.3
4.61	0.496	0.8661	21.6
5.00	0.544	0.8669	23.1
5.32	0.585	0.8672	24.6
5.70	0.628	0.8672	26.5
6.02	0.682	0.8658	29.8
6.32	0.738	0.8619	34.7
6.75	0.804	0.8530	44.1
6.95	0.842	0.8388	53.8
7.44	0.913	0.7967	96.4

signed so that a single charge of fluid may be employed for measurements of the liquid phase density and level. Parts of the apparatus requiring precise temperature control were housed in a commercial air oven (A) equipped

Table 3. Mole Fraction, Liquid Density, and Liquid Volume of CO_2 (1) + *N,N*-Dimethylformamide (2) at 290.8, 300.9, and 310.1 K

P/MPa	x_1	ϱ_L/(g·cm^{-3})	V_L/cm^3
	T = 290.8 K		
0.78	0.071	0.9620	15.6
1.48	0.133	0.9703	16.1
2.20	0.256	0.9784	17.6
2.55	0.329	0.9822	18.8
2.91	0.384	0.9854	19.9
3.26	0.469	0.9883	22.2
3.60	0.533	0.9903	24.4
3.94	0.604	0.9912	27.6
4.29	0.668	0.9896	31.9
4.64	0.743	0.9833	39.9
4.95	0.817	0.9685	54.5
5.17	0.871	0.9478	76.3
5.30	0.897	0.9318	97.2
	T = 300.8 K		
1.56	0.074	0.9538	15.5
2.16	0.137	0.9628	16.1
2.58	0.186	0.9662	16.6
2.94	0.264	0.9689	17.7
3.25	0.328	0.9710	18.8
3.60	0.398	0.9731	20.3
3.91	0.448	0.9744	21.6
4.26	0.501	0.9755	23.2
4.60	0.556	0.9755	25.4
4.96	0.628	0.9740	29.3
5.30	0.679	0.9703	33.1
5.65	0.746	0.9606	40.7
5.99	0.804	0.9468	51.8
6.22	0.855	0.9248	69.4
6.48	0.893	0.8992	95.0
	T = 310.1 K		
1.40	0.080	0.9404	15.7
2.20	0.132	0.9490	16.1
2.66	0.188	0.9516	16.8
2.95	0.222	0.9533	17.2
3.28	0.260	0.9551	17.7
3.60	0.309	0.9567	18.6
3.96	0.352	0.9581	19.4
4.30	0.413	0.9593	20.8
4.66	0.463	0.9600	22.1
4.98	0.508	0.9603	23.6
5.32	0.544	0.9599	25.1
5.64	0.587	0.9589	27.1
5.95	0.624	0.9567	29.2
6.37	0.670	0.9526	32.7
6.66	0.714	0.9458	37.0
7.11	0.770	0.9354	45.1
7.37	0.816	0.9166	56.0
7.61	0.859	0.8937	73.0
7.82	0.891	0.8689	95.0

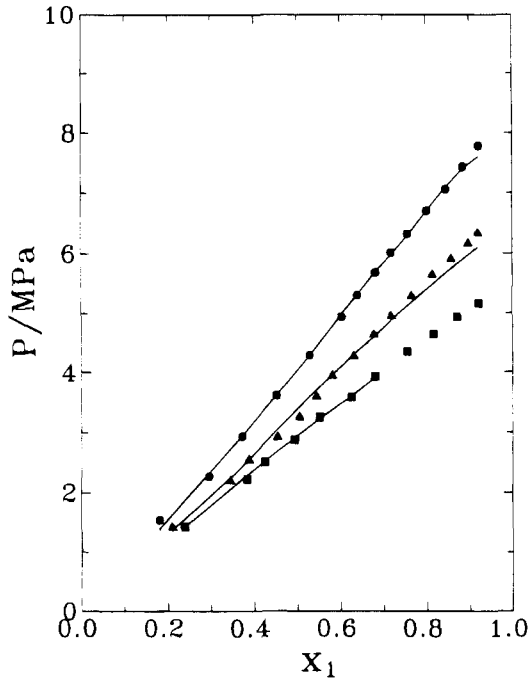

Figure 2. Comparison of the calculated mole fraction x_1 of carbon dioxide (1) + cyclohexanone (2) with experimental data at different temperatures: (■) 290.8 K, (▲) 300.9 K, (●) 310.1 K, (−) calculated with the PT-EOS.

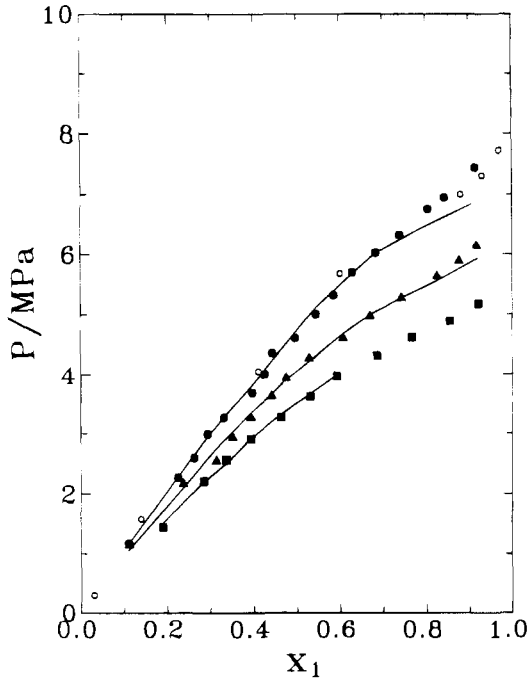

Figure 3. Comparison of the calculated mole fraction x_1 of carbon dioxide (1) + toluene (2) with experimental data at different temperatures: (■) 290.8 K, (▲) 300.9 K, (●) 310.1 K, (○) 311 K, Ng and Robinson (*9*), (−) calculated with the PT-EOS.

with a high-pressure see-through windowed Jerguson cell (B), the vibrating U-tube portion of a digital density meter (C), a storage cylinder (D), and a magnetic recirculation pump (E). The magnetic pump recirculated liquid through the U-tube of the density meter.

The Jerguson cell employed a standard metal rule to measure the liquid level up to 15 cm with a precision of 0.05 cm. The liquid phase density was measured by using an Anton/Paar vibrating tube densitometer with a resolution of 0.0001 g/cm^3. System pressures were measured with a digital pressure transducer (F) and checked by a Bourdon tube gauge (G). The temperature in the oven was

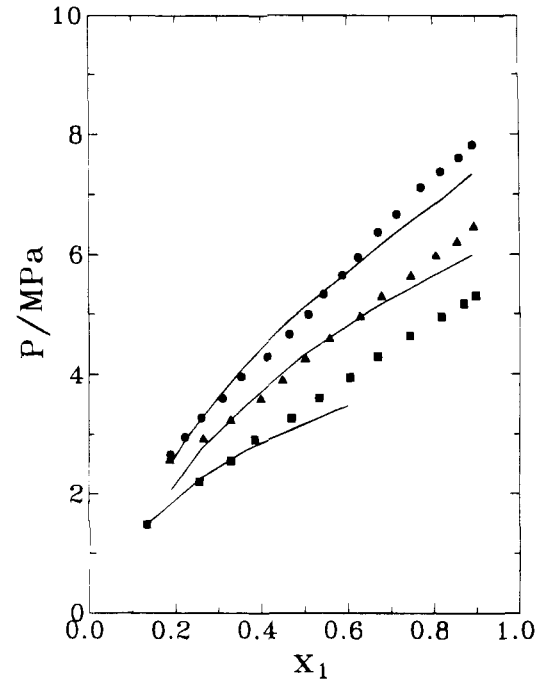

Figure 4. Comparison of the calculated mole fraction x_1 of carbon dioxide (1) + *N*,*N*-dimethylformamide (2) with experimental data at different temperatures. Symbols as in Figure 2.

Table 4. Mole Fraction, Liquid Density, and Liquid Volume of N_2O (1) + Cyclohexanone (2) at 290.8, 300.9, and 310.1 K

P/MPa	x_1	ϱ_L/(g·cm^{-3})	V_L/cm^3
		T = 290.8 K	
1.40	0.321	0.9553	18.0
1.82	0.392	0.9576	19.1
2.16	0.450	0.9598	20.2
2.55	0.508	0.9619	21.6
2.91	0.570	0.9634	23.5
3.26	0.625	0.9643	25.7
3.60	0.680	0.9643	28.7
3.94	0.744	0.9618	34.0
4.29	0.807	0.9538	42.8
4.61	0.869	0.9371	60.4
4.91	0.918	0.9111	93.8
		T = 300.9 K	
1.46	0.256	0.9454	17.2
2.18	0.375	0.9484	18.8
2.57	0.413	0.9498	19.5
2.93	0.468	0.9509	20.7
3.27	0.506	0.9518	21.6
3.58	0.563	0.9522	23.4
3.94	0.617	0.9519	25.5
4.30	0.671	0.9502	28.4
4.62	0.721	0.9470	32.1
4.97	0.775	0.9400	38.1
5.29	0.826	0.9297	47.4
5.60	0.877	0.9064	65.1
5.93	0.918	0.8814	95.7
		T = 310.1 K	
1.51	0.245	0.9351	17.1
2.30	0.331	0.9373	18.2
2.94	0.405	0.9388	19.4
3.60	0.475	0.9397	20.9
3.94	0.523	0.9398	22.1
4.28	0.564	0.9394	23.5
4.60	0.604	0.9387	25.0
4.97	0.646	0.9370	27.1
5.34	0.691	0.9336	30.0
5.69	0.734	0.9302	33.5
6.01	0.778	0.9214	38.9
6.35	0.822	0.9084	47.2
6.71	0.870	0.8828	63.4
6.99	0.898	0.8601	80.4
7.18	0.917	0.8466	97.9

regulated by a commercial temperature controller and measured by a platinum resistance thermometer with

Table 5. Mole Fraction, Liquid Density, and Liquid Volume of N_2O (1) + Toluene (2) at 290.8, 300.9, and 310.1 K

P/MPa	x_1	ϱ_L/(g·cm^{-3})	V_L/cm^3
	T = 290.8 K		
1.50	0.254	0.8792	17.2
2.15	0.381	0.8854	19.0
2.51	0.456	0.8888	20.5
2.93	0.544	0.8929	22.9
3.30	0.620	0.8960	25.8
3.62	0.689	0.8979	29.9
3.95	0.765	0.8974	37.0
4.27	0.829	0.8923	48.4
4.57	0.883	0.8819	67.8
4.85	0.920	0.8697	97.2
	T = 300.9 K		
1.58	0.189	0.8690	16.5
2.22	0.278	0.8730	17.5
2.55	0.344	0.8751	18.4
2.90	0.410	0.8774	19.6
3.24	0.466	0.8791	20.8
3.60	0.540	0.8810	22.8
3.93	0.602	0.8822	25.2
4.26	0.665	0.8823	28.4
4.63	0.729	0.8806	33.4
4.97	0.796	0.8738	42.2
5.31	0.859	0.8599	58.4
5.73	0.920	0.8300	100.3
	T = 310.1 K		
1.51	0.158	0.8569	16.2
2.29	0.238	0.8598	17.0
2.98	0.326	0.8627	18.2
3.62	0.421	0.8651	19.8
3.96	0.474	0.8661	21.1
4.32	0.531	0.8668	22.6
4.60	0.569	0.8668	24.0
5.00	0.622	0.8661	26.3
5.38	0.680	0.8648	29.7
5.75	0.727	0.8612	33.6
6.08	0.786	0.8499	41.3
6.35	0.826	0.8393	49.6
6.71	0.871	0.8203	65.5
7.13	0.913	0.7999	95.6

digital readout (H). The temperature of the Jerguson cell was monitored by a thermocouple and a digital temperature indicator (I). The vibrating U-tube in a controlled constant temperature bath with digital readout (J) is monitored by a high-precision thermometer (K).

Liquid solvent was charged volumetrically into the cell and degassed by evacuating the whole apparatus; then sufficient gas was injected through a feed-forward regulator (L) to give the desired pressure. The magnetic pump was then operated until equilibrium, as indicated by repeated constant density readings of the liquid phase. Equilibrium times ranged from approximately 1/2 h at lower pressures to 2 h at higher pressures.

When equilibrium was established, the density and level of the liquid phase were measured for two or three successive readings to check for consistency of equilibrium. This procedure was repeated at a series of pressures. The density of the liquid phase ϱ was calculated by means of the well-known relation of Albert et al. (*23*)

$$\varrho = \varrho_0 + K_p(\tau^2 - \tau_0^2) \quad (1)$$

where the subscript zero refers to a reference liquid. The densitometer constant K_p is determined from the period of vibration (τ) of distilled water and nitrogen of accurately known densities. The liquid volume of the equilibrium cell V_L can be expressed by an increased level of the liquid phase ΔL:

$$V_L = V_p + A\delta L \quad (2)$$

where V_p is the volume occupied by the pure solvent and

Table 6. Mole Fraction, Liquid Density, and Liquid Volume of N_2O (1) + *N,N*-Dimethylformamide (2) at 290.8, 300.9, and 310.1 K

P/MPa	x_1	ϱ_L/(g·cm^{-3})	V_L/cm^3
	T = 290.8 K		
1.44	0.208	0.9602	17.2
2.22	0.314	0.9653	18.8
2.58	0.357	0.9671	19.7
2.93	0.418	0.9697	21.1
3.29	0.478	0.9716	22.7
3.64	0.544	0.9727	25.2
4.00	0.612	0.9726	28.6
4.34	0.694	0.9687	34.8
4.64	0.788	0.9554	48.3
4.86	0.860	0.9313	71.9
5.03	0.893	0.9154	94.1
	T = 300.9 K		
1.53	0.186	0.9498	16.9
2.31	0.281	0.9537	18.3
2.58	0.313	0.9498	18.8
2.93	0.350	0.9565	19.5
3.27	0.391	0.9579	20.4
3.64	0.435	0.9591	21.5
3.97	0.494	0.9599	23.3
4.33	0.542	0.9603	25.2
4.66	0.598	0.9596	27.9
5.00	0.653	0.9575	31.5
5.34	0.719	0.9494	37.8
5.66	0.806	0.9290	53.2
5.87	0.860	0.9140	72.6
6.02	0.894	0.8870	96.4
	T = 310.1 K		
1.58	0.141	0.9389	16.4
2.29	0.208	0.9416	17.2
2.97	0.271	0.9437	18.2
3.65	0.341	0.9454	19.4
3.96	0.391	0.9464	20.5
4.32	0.430	0.9469	21.5
4.65	0.477	0.9471	24.3
4.99	0.518	0.9468	26.1
5.37	0.560	0.9462	26.1
5.73	0.605	0.9435	28.5
6.06	0.645	0.9421	31.2
6.43	0.699	0.9349	35.9
6.72	0.762	0.9210	44.5
7.01	0.822	0.8927	59.3
7.31	0.890	0.8569	95.6

A is the cross area of the equilibrium cell, which was determined by the changing level of a certain amount of water. Then, the experimental solubility of gas in the liquid phase could be obtained from the weight of gas in the liquid phase W_L, which is the difference between the weight of the liquid phase at each pressure $(\varrho V)_L$ and the weight of the pure solvent $(\varrho V)_p$ according to

$$W_L = (\varrho V)_L - (\varrho V)_p \quad (3)$$

The only assumption is that the evaporation of solvents into the vapor phase is small enough to be neglected. The error in composition due to the loss of the heavy component (solvent) in the vapor phase was estimated within 0.01 mole fraction. This has been evidenced by using an equation of state to calculate the vapor phase composition. The total error in the calculation of the liquid phase composition, due to the assumption and the error in measuring the liquid level, was smaller than 0.05 mole fraction. The accuracy of the experimental data (i.e., mole fraction of CO_2 in the liquid phase) is within 2%, when compared with the data of Ng and Robinson (1978). Uncertainties in all measurements were evaluated by measuring temperatures with an error of less than 0.1 K, which were calibrated by a high-precision thermometer (Hart Scientific, 1506), and pressures with an error of 0.5 psi in the range below 1000 psi and 2 psi above 1000 psi.

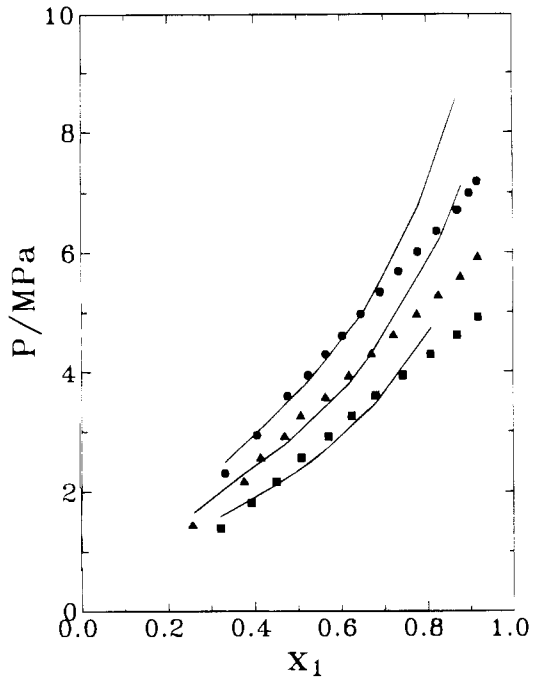

Figure 5. Comparison of the calculated mole fraction x_1 of nitrous oxide (1) + cyclohexanone (2) at different temperatures: (■) 290.8 K, (▲) 300.9 K, (●) 310.1 K, (—) calculated with the PT-EOS.

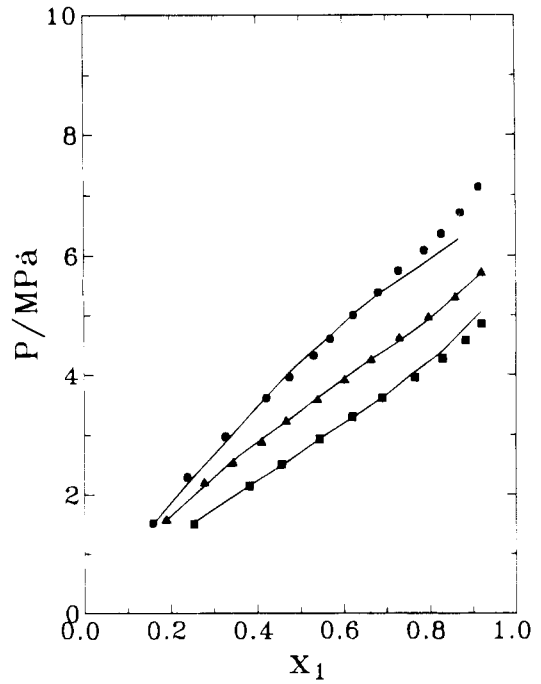

Figure 6. Comparison of the calculated mole fraction x_1 of nitrous oxide (1) + toluene (2) at different temperatures. Symbols as in Figure 5.

Materials

The gases CO_2 and N_2O used in these studies were supplied by a local Air Product Division and had a stated purity of 99.5+%. The toluene, cyclohexanone, and *N,N*-dimethylformamide were from Merck Chemical Co. with a stated purity of 99.5+%. The chemicals were used without further purification.

Results and Discussion

Tables 1–3 give the unsmoothed data (x_1, ϱ_L, V_L) for CO_2 + cyclohexanone, CO_2 + toluene, and CO_2 + *N,N*-dimethylformamide, respectively, over the temperature range from

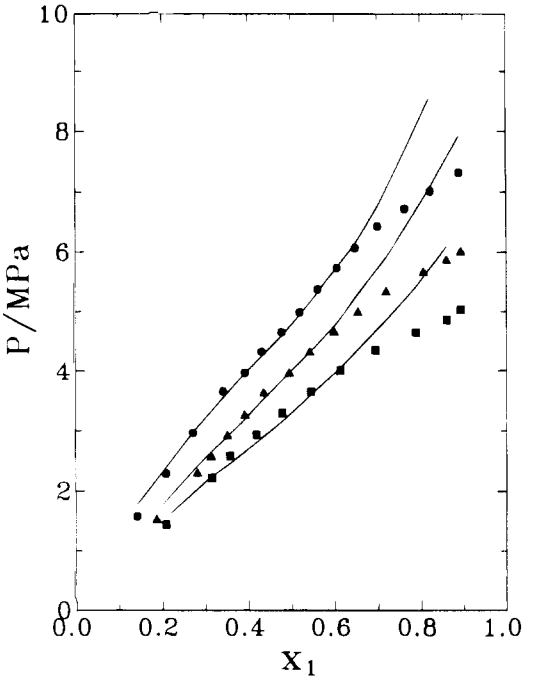

Figure 7. Comparison of the calculated mole fraction x_1 of nitrous oxide (1) + *N,N*-dimethylformamide (2) at different temperatures. Symbols as in Figure 5.

Table 7. Binary Interaction Parameter for the PT-EOS for Carbon Dioxide + Solvent and Nitrous Oxide + Solvent[a]

		CO_2			N_2O		
		290.8 K	300.9 K	310.1 K	290.8 K	300.9 K	310.1 K
CX	k_{12}	0.017	0.008	0.006	−0.115	−0.103	−0.100
	k_{21}	0.035	0.016	0.013	0.007	0.008	0.011
		(0.79)	(2.27)	(1.16)	(6.04)	(8.81)	(7.54)
TOL	k_{12}	0.133	0.139	0.151	0.057	0.083	0.114
	k_{21}	0.188	0.201	0.204	0.141	0.196	0.191
		(1.56)	(2.65)	(2.33)	(1.57)	(0.71)	(2.12)
DMF	k_{12}	0.009	0.042	0.037	−0.052	−0.052	−0.055
	k_{21}	0.150	0.141	0.132	0.021	0.024	0.050
		(5.62)	(4.63)	(3.69)	(7.23)	(7.54)	(4.83)

[a] CX = cyclohexanone, TOL = toluene, DMF = *N,N*-dimethylformamide. The values in parentheses are the average absolute deviations in $\Delta P/P$: $AAD(\Delta P/P)/\% = (100/n)\sum_{k=1}^{n}[|(P^{calcd} - P^{exptl})/P^{exptl}|]_k$.

290.8 to 310.1 K, with plots in Figures 2–4. The data for N_2O + cyclohexanone, N_2O + toluene, and N_2O + *N,N*-dimethylformamide at the same temperatures are shown in Tables 4–6 and Figures 5–7, respectively.

The solubility at 0.1 MPa is unmeasured at all temperatures. It can be seen that the solubilities of carbon dioxide in the liquid phase for three solvents are less than those of nitrous oxide. At the same pressure, both gases have greater solubilities in cyclohexanone than in toluene and in *N,N*-dimethylformamide. When the N_2O + cyclohexanone data at 290.8 and 300.9 K in this study are compared with those of Rusz et al. (*24*) at 293.15 K, the values of the latter appear to fall between the present data at 291.8 and 300.9 K.

The data were fit with the Patel–Teja equation of state (PT-EOS) with a composition dependent mixing rule. The PT-EOS can be written as (*25*)

$$P = \frac{RT}{v - b} - \frac{a}{v(v + b) + c(v - b)} \tag{4}$$

where P is the pressure, T is the temperature, R is the gas constant, v is the molar volume, and a, b, and c are the temperature dependent parameters. The van der Waals

one-fluid mixing rules, a nonquadratic mixing rule for a and a linear function of mole fraction in the combining rule for a_{ij} (26), were used to calculate the mixture parameters:

$$a = \sum\sum x_i x_j a_{ij} \quad (5)$$

$$b = \sum x_i b_i \quad (6)$$

$$c = \sum x_i c_i \quad (7)$$

$$a_{ij} = (a_i a_j)^{0.5}[1 - k_{ij} + (k_{ij} - k_{ji})x_i] \quad (8)$$

The two adjustable binary interaction parameters, k_{ij} and k_{ji}, were obtained by fitting the data with the temperature and pressure as the independent variables and minimizing the error in the liquid composition. Table 7 shows the binary interaction parameters obtained in this study for CO_2 + solvent and N_2O + solvent systems.

Generally speaking, phase equilibrium compositions can be correlated quite well with the one-fluid mixing rules of van der Waals, but for mixtures containing molecules dissimilar in size or chemical nature, the correlated phase compositions would not be in good agreement with experiment. As suggested by Panagiotopoulos and Reid (26), this study using the composition dependent mixing rule with two adjustable binary parameters, k_{12} and k_{21}, gave a fair correlation of liquid phase composition for CO_2 + cyclohexanone, CO_2 + toluene, and CO_2 + *N*,*N*-dimethylformamide, shown in Figures 2–4. However, the same mixing rule correlated rather poorly for the liquid phase composition in mixtures of N_2O + cyclohexanone and N_2O + *N*,*N*-dimethylformamide; the values of the average absolute deviation of pressure, i.e., AAD($\Delta P/P$)/% was shown in Table 7. It might be possible that much larger dipole moments of cyclohexanone and *N*,*N*-dimethylforamide than N_2O cause the deviation of correlation for these two mixtures of relatively asymmetric molecules.

Literature Cited

(1) McHugh, M. A.; Krukonis, V. J. *Supercritical Fluid Extraction: Principles and Practice*; Butterworths: Boston, MA, 1986.
(2) Paulaitis, M. E.; Penninger, J. M. L.; Gray, R. D.; Davidson, P. *Chemical Engineering at Supercritical Fluid Conditions*; Ann Arbor Science: Ann Arbor, MI, 1983.
(3) Johnston, K. P.; Penninger, J. M. L. *Supercritical Fluid Science and Technology*; ACS Symposium Series 406; American Chemical Society: Washington, DC, 1989.
(4) Prausnitz, J. M.; Lichtenthaler, R. N.; deAzevedo, E. G. *Molecular Thermodynamics of Fluid-Phase Equilibria*; Prentice Hall: Englewood Cliffs, NJ, 1986.
(5) Squires, T. G.; Paulaitis, M. E. *Supercritical Fluids: Chemical and Engineering Principles and Applications*; ACS Symposium Series 329; American Chemical Society: Washington, DC, 1987.
(6) Elgin, J. C.; Weinstock, J. J. *J. Chem. Eng. Data* **1959**, *4*, 3–9.
(7) Katayama, T.; Ohgaki, K.; Maekawa, G.; Goto, M.; Nagano, T. *J. Chem. Eng. Jpn.* **1975**, *8*, 89–92.
(8) Weber, W.; Zeck, S.; Knapp, H. *Fluid Phase Equilib.* **1984**, *18* (3), 253–278.
(9) Ng, H. J.; Robinson, D. B. *J. Chem. Eng. Data* **1978**, *23*, 325–342.
(10) Morris, W. O.; Donohue, M. D. *J. Chem. Eng. Data* **1985**, *30*, 259–264.
(11) Sebastian, H. M.; Simnick, J. J.; Lin, H. M.; Chao, K. C. *J. Chem. Eng. Data* **1980**, *25*, 246–252.
(12) Fink, S. D.; Hershey, H. C. *Ind. Eng. Chem. Res.* **1990**, *29*, 295–306.
(13) Baumgaertner, M.; Moorwood, R. A. S.; Wenzel, H. In *Thermodynamics of Aqueous Systems with Industrial Applications*; Newman, S. A., Ed.; ACS Symposium Series 133; American Chemical Society: Washington, DC, 1980; pp 415–434.
(14) Clever, H. L.; Han, C. H. In *Thermodynamics of Aqueous Systems with Industrial Applications*; Newman, S. A., Ed.; ACS Symposium Series 133; American Chemical Society: Washington, DC, 1980; pp 513–536.
(15) Japas, M. L.; Franck, E. U. *Ber. Bunsen-Ges. Phys. Chem.* **1985**, *89*, 1268–1275.
(16) Mather, A. E.; Franck, E. U. *J. Phys. Chem.* **1992**, *96*, 6–8.
(17) Adams, W. R.; Zollweg, J. A.; Streett, W. B.; Rizvi, S. S. H. *AIChE J.* **1988**, *34* (8), 1387–1391.
(18) Foster, N. R.; Macnaughton, S. J.; Chaplin, R. P.; Wells, P. T. *Ind. Eng. Chem. Res.* **1989**, *28*, 1903–1907.
(19) King, M. B.; Anderson, D. A.; Fallah, F. H.; Kassim, D. M.; Kassim, K. M.; Sheldon, J. R.; Mahmud, R. S. In *Chemical Engineering at Supercritical Fluid Conditions*; Paulaitis, M. E., Eds.; Ann Arbor Science: Ann Arbor, MI, **1983**; pp 31–79.
(20) Kato, M.; Aizawa, K.; Kanahira, T.; Ozawa, T. *J. Chem. Eng. Jpn.* **1991**, *24*, 767–771.
(21) Robinson, R. L., Jr.; Nagarajan, N. *J. Chem. Eng. Data* **1987**, *32*, 369–371.
(22) Chang, C. J. *Fluid Phase Equilib.* **1992**, *74*, 235–242.
(23) Albert, H. J.; Gates, J. A.; Wood, R. H.; Grolier, J. E. *Fluid Phase Equilib.* **1985**, *20*, 321–330.
(24) Rusz, L.; Makranczy, J.; Balog-Megyery, K.; Patyi, L. *Hung. J. Ind. Chem.* **1977**, *5*, 225–232.
(25) Patel, N. C.; Teja, A. S. *Chem. Eng. Sci.* **1982**, *37*, 463–473.
(26) Panagiotopoulos, A. Z.; Reid, R. C. In *Equation of State Theories and Applications*; Chao, K. C., Ed.; ACS Symposium Series 300; American Chemical Society: Washington, DC, 1986; pp 571–582.

Received for review November 14, 1994. Revised January 31, 1995. Accepted March 5, 1995.[⊗] Acknowledgment is made to the National Science Council of the Republic of China (Grant No. NSC 82-0402-E005-001) for financial support of this work.

JE9402435

[⊗] Abstract published in *Advance ACS Abstracts*, May 1, 1995.